

# Electron transport in nitrogen-polar high electron mobility transistors

David F. Brown<sup>\*</sup>, Siddharth Rajan, Stacia Keller, Yun-Hao Hsieh, Steven P. DenBaars, and Umesh K. Mishra

Department of Electrical and Computer Engineering, University of California, Santa Barbara CA, 93106, USA

Received 9 September 2008, accepted 10 February 2009

Published online 20 March 2009

PACS 72.20.Dp, 72.20.Fr, 73.40.Kp, 73.61.Ey, 85.30.De, 85.30.Tv

<sup>\*</sup> Corresponding author: e-mail [dfbrown@ece.ucsb.edu](mailto:dfbrown@ece.ucsb.edu), Phone: 1-805-893-3812, Fax: 1-805-893-8714

The electron mobility in N-polar heterostructures was measured as a function of gate bias using resistance and capacitance measurements on gated transmission line method structures. The mobility was observed to decrease as the gate was reverse biased. Experimental results also revealed that the access resistance of the device increased with increasing reverse bias of the gate. Theoretical scattering rates caused by pho-

non, alloy disorder and ionized impurity scattering were calculated as a function of gate bias and found to match the experimental data well. An electrostatic model was developed to calculate the sheet charge density of the devices, and they were found to be independent of the polarization of the barrier layer.

© 2009 WILEY-VCH Verlag GmbH & Co. KGaA, Weinheim

**1 Introduction** N-polar nitride semiconductors are very promising because the reversal of the polarization charges allows for novel device structures [1]. In GaN/AlGaN/GaN structures, these polarization charges lead to a fixed sheet of mobile electrons, or a two-dimensional electron gas (2DEG), at the top heterointerface, which forms the basis of N-polar high electron mobility transistors (HEMTs) [2-4]. These N-Polar devices have a different band structure than typical Ga-polar HEMTs, which leads to unique transport properties which are not observed in Ga-polar devices [4, 5].

In this study, the low-field transport characteristics of N-polar HEMTs grown by metal organic chemical vapour deposition (MOCVD) were studied. The sheet charge density, drift mobility, and access resistance were measured as a function of gate bias using capacitance-voltage (C-V) and resistance measurements on gated transmission line method (TLM) structures. A theoretical model was developed to calculate the sheet charge density, as well as the electron mobility in these devices limited by optical phonon, alloy disorder, and ionized impurity scattering. The measured drift mobility was found to match the theoretical values well.

**2 Experiment** The HEMT structure measured in this experiment was grown by MOCVD on a sapphire substrate with a 3 degree miscut towards the a-plane. The growth process is described in detail in a previous study [4]. A schematic of the device structure used in this experiment is shown in Fig. 1.

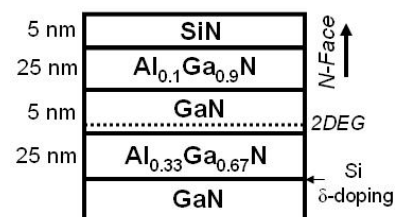


**Figure 1** Epitaxial structure of the N-Polar HEMT used in this study.

The channel layer of the device is capped with 25 nm of  $\text{Al}_{0.1}\text{Ga}_{0.9}\text{N}$  and 5 nm of SiN grown in-situ by MOCVD. These layers have been experimentally shown to reduce the gate leakage significantly [3, 4].

Measurements were done on gated-TLM structures, through which we extracted the sheet charge density, mobility, and access resistance as a function of gate bias. The

structures were oriented parallel to the direction of the substrate miscut, because the measured mobility is anisotropic with respect to the direction of the source current [4]. Gate lengths varied from 2  $\mu\text{m}$  to 20  $\mu\text{m}$  while the access region lengths were constant at 2  $\mu\text{m}$ . The 2DEG Sheet charge  $n_s$  under the gate was measured using a C-V measurement. The varying gate lengths employed corresponded to the set of spacings common in TLM measurements. A small current of 25  $\mu\text{A}$  was used for the resistance measurement in order to avoid pinch-off of the channel and other high-field effects. The drift mobility as a function of gate bias can then be easily calculated using Eq. (1).

$$\mu(V_G) = [eR_{sh}(V_G)n_s(V_G)]^{-1} \quad (1)$$

### 3 Theory

**3.1 Electron wave function** The wave function for electrons in the 2DEG is needed for accurate evaluation of transport properties and scattering rates. As a first approximation, an infinite triangular well was assumed, where the electric field in the channel is unaffected by the 2DEG charge. The wave function used is shown in Eq. (2), where  $a$  and  $b$  are variational parameters, and  $C$  is a normalization constant.

$$\psi(z) = Cz^a \exp(-bz/2), z \geq 0 \quad (2)$$

$$C = \sqrt{\frac{b^{2a+1}}{\Gamma(2a+1)}} \quad (3)$$

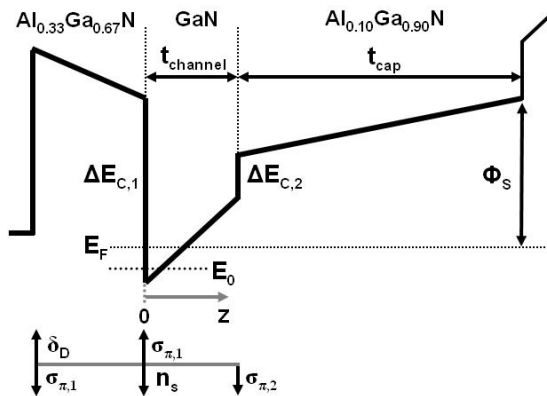


**Figure 2** Conduction band diagram and the relevant charges of the N-Polar HEMT used in this experiment. The N-face is on the right side.

Using this as a trial function, the first sub-band energy  $E_0$  can be obtained. Further minimization of  $E_0$  yields the parameter  $b$  [6]:

$$E_0 = \frac{\hbar^2}{2m_w^*} \frac{b^2}{4(2a-1)} + \frac{eF_C}{b} (2a+1) \quad (4)$$

$$b^3 = 4e\hbar^{-2} m_w^* F_C (2a+1)(2a-1) \quad (5)$$

where  $m_w^*$  is the effective mass in the channel and  $F_C$  is the electric field in the channel. Finally, minimization of  $b$  yields  $a = 1.5$ .  $F_C$  at zero gate bias can be easily calculated from the band diagram in figure 2 if the channel charge at zero bias is known, and has been done in detail in an earlier study [5]. The charge  $n_s(0)$  measured by C-V was used in the calculations. It follows that for an arbitrary gate bias,  $F_C(V_G) = F_C(0) + V_G/(t_C + t_{cap} + t_{SiN})$ , and  $n_s(V_g)$  can be calculated using Poisson's equation.

**3.2 Sheet charge density** The electron sheet charge density of an N-polar HEMT structure can be calculated using an electrostatic model derived from the band diagram in Fig. 2. We made two simplifying assumptions: (1) the electric field below the AlGa<sub>N</sub> barrier layer is zero, and (2) no charges are at the hetero-interfaces aside from the 2DEG, polarization charges, and intentional dopants.

The second assumption is important, because the Fermi level at the back hetero-interface of the barrier layer will approach the valence band, which will lead to ionized donor traps or hole accumulation at this interface. To counter this, a silicon delta-doping with a density of approximately  $\delta_D = 8 \times 10^{12} \text{ cm}^{-2}$  is typically introduced at this interface during growth.

Using Poisson's equation and the band diagram in Fig. 2, we obtained the following equations:

$$F_B = [e\delta_D - \sigma_{\pi,1}] / \epsilon \quad (6)$$

$$F_C = F_B + [\sigma_{\pi,1} - en_s] / \epsilon \quad (7)$$

$$F_{cap} = F_C + \sigma_{\pi,2} / \epsilon \quad (8)$$

$$F_C t_C + \Delta E_{C,2} + F_{cap} t_{cap} = \phi_S + E_0 + (E_F - E_0) \quad (9)$$

where  $F_B$  is the electric field in the barrier,  $F_{cap}$  is the electric field in the cap,  $\sigma_{\pi,1}$  and  $\sigma_{\pi,2}$  are the net polarization charges at the barrier-channel and channel-cap interfaces respectively,  $\epsilon$  is the permittivity and  $\Phi_S$  is the surface potential.  $\Phi_S$  has been measured as approximately 1 eV for GaN with C-V measurements [7]. 1.1 eV is a reasonable estimate for Al<sub>0.1</sub>Ga<sub>0.9</sub>N.

It is interesting to note that after substituting equation 5 into Eq. (7) that the parameter  $\sigma_{\pi,1}$  cancels, meaning that the sheet charge density does not depend on polarization from the AlGa<sub>N</sub> barrier. Instead, the key contributors to the 2DEG charge are the delta doping density and the thickness of the channel and the cap. Furthermore, the polarization charge at the channel-cap interface will deplete the 2DEG. The sheet charge density can then be obtained by solving the equations for  $n_s$ .

This model does not account for significant level of oxygen impurities in the device (which will be discussed in detail later). For this reason, the 2DEG charge used in the calculations for this experiment was measured.

## 4 Scattering mechanisms

**4.1 Polar optical phonon** Electron mobility in III-nitride heterostructures is typically limited by optical phonon scattering at temperatures greater than 100 K. An analytical expression has been derived by Gelmont, Shur, and Strosio which was used for our calculation [8]:

$$\frac{1}{\tau_{op}} = \frac{e^2 \omega_{op} m_w^* N_B(T) G(b, q_0)}{2 \varepsilon^* q_0 \hbar^2 F(y)} \quad (10)$$

In Eq. (10),  $N_B(T)$  is the Bose-Einstein distribution function,  $q_0$  is the optical phonon wave vector where  $q_0 = \sqrt{2m_w^* (\hbar \omega_{pop})} / \hbar$ , and  $G(b, q_0)$  is the form factor for the wave function, which for the wave function in Eq. (2) with  $a=1.5$  is

$$G(b, q) = \frac{9b(16b^3 + 29b^2q + 20bq^2 + 5q^3)}{144(b+q)^4} \quad (11)$$

$F(y)$  is given by

$$F(y) = 1 + \frac{1 - e^{-y}}{y} \quad (12)$$

where  $y$  is a dimensionless variable.

$$y = \frac{\pi \hbar^2 n_s}{m_w^* k_B T} \quad (13)$$

**4.2 Alloy disorder** Alloy disorder scattering, resulting from wave function penetration into the barrier, has been shown to be very large in Ga-polar AlGaIn/GaN HEMTs due to the large conduction band offset between binary AlN and GaN, resulting in a large scattering potential. The wave function in Eq. (2) does not account for barrier penetration, but it can be easily modified [5]. The modified wave function is

$$\psi(z) = M \exp(\kappa_B z / 2), z < 0 \quad (14)$$

$$\psi(z) = N C (z + z_0)^a \exp(-bz/2), z \geq 0 \quad (15)$$

$$\kappa_B = 2\hbar^{-1} \sqrt{2m_b^* (\Delta E_{C,1} - E_0)} \quad (16)$$

The constants  $z_0$ ,  $M$ , and  $N$  can be obtained by matching boundary conditions.

$$z_0 = 2a(\kappa_B + b)^{-1} \quad (17)$$

$$N = \sqrt{\frac{\kappa_B}{\kappa_B e^{bz_0} + C^2 z_0^{2a}}} \quad (18)$$

$$M = N C z_0^a \quad (19)$$

With the modified wave function, the integrated probability of finding an electron in the barrier is

$$P_B = \frac{M^2}{\kappa_B} \quad (20)$$

The alloy scattering rate for 2DEGs has been derived by Bastard as [9]

$$\frac{1}{\tau_{alloy}} = \frac{m_b^* \Omega V_A^2 x(1-x)}{e^2 \hbar^3} \times \frac{\kappa_B P_B^2}{2} \quad (21)$$

With  $\Omega$  as the unit cell volume,  $V_A$  as the alloy scattering potential, which has been measured as 1.8 V for AlGaIn with magnetotransport measurements [10], and  $x$  as the alloy composition.

**4.3 Ionized impurity** An undesirable consequence of the MOCVD growth of N-polar films is an increased incorporation of oxygen impurities [11]. Through optimization of growth conditions, the density of background impurities in GaN can be decreased to approximately  $10^{17} \text{ cm}^{-3}$ . However, due to the increased affinity of aluminium for oxygen, the oxygen concentration in AlGaIn films has been measured to be as high as  $3.5 \times 10^{18} \text{ cm}^{-3}$  with both SIMS and C-V measurements [7].

There are several models which can be used to calculate the impurity scattering rate. One is to treat the impurities in the barrier as remote impurities, with the distance of the wave function from the barrier being used as the separation of the 2DEG to the impurities. This calculation is very straightforward, but will underestimate the lifetime because the wave function does not account for barrier penetration. However, this is expected to be accurate at low gate bias where barrier penetration is minimal. The scattering rate for remote ionized impurities in the barrier layer is [12]

$$\frac{1}{\tau_{ri}} = \frac{m_w^* N_{imp}^{3D}}{4\pi \hbar^3 k_F^3} \left( \frac{e^2}{2\varepsilon} \right)^{2k_F} \int_0^{2k_F} \frac{F(b, q)^2}{[q + q_{TF} G(b, q)]^2} \frac{q dq}{\sqrt{1 - (q/2k_F)^2}} \quad (22)$$

where  $k_F$  is the Fermi wave vector,  $q_{TF}$  is the Thomas-Fermi wave vector, and  $d$  is the spacing between the 2DEG centroid and the barrier.  $F(b, q)$  is a form factor, and is given by

$$F(b, q) = \left( \frac{b}{b+q} \right)^{2a+1} \quad (23)$$

As the gate is reverse biased, barrier penetration is significant, so where it may be more accurate to model the impurities as background dopants for the electrons within the barrier. By adapting our wave function to an estimate for the scattering rate given by Davies [12], we obtained

$$\frac{1}{\tau_{bi}} \approx N_{imp}^{3D} \frac{m_b^* P_B^2}{2\pi \hbar^3 k_F^3} \left( \frac{e^2}{2\varepsilon} \right)^2 \quad (24)$$

There is approximately one order of magnitude difference between these two models when the gate is biased near pinch-off.

**5 Results** The theoretical mobility is easily calculated using Matheson's rule and the Drude relation. Figure 3

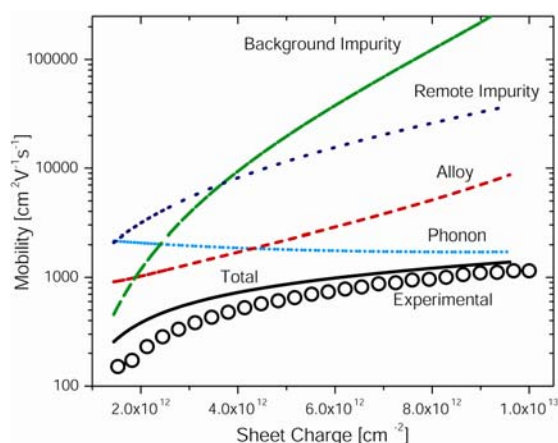


**Figure 3** Theoretical and experimental values of mobility plotted vs. 2DEG sheet charge as the device is pinched off.

shows the calculated mobility as a function of sheet charge in the channel as the device is pinched off, along with the mobility limited by each of the scattering mechanisms. At zero bias, the experimentally measured charge and mobility are  $9.7 \times 10^{12} \text{ cm}^{-2}$  and  $1150 \text{ cm}^2 \text{ V}^{-1} \text{ s}^{-1}$  respectively.

The mobility is limited by optical phonon scattering at low gate bias, but alloy scattering has an increasing impact as the barrier penetration of the wave function increases with increasing gate bias. As the field increases further, impurity scattering becomes important as barrier penetration increases and screening is reduced due to the decrease in charge density. Both the shape and the values of the theoretical curve had a good fit to the data collected experimentally, although temperature-dependent measurements should be done to verify that impurity scattering is dominant near pinch-off, as the 2DEG may be more weakly degenerate at lower charge densities and high temperature.

As shown in Fig. 4, the access resistance of the device was observed to increase with an increasing reverse bias of the gate. More research is being done to understand this phenomenon, but we speculate that the difference in the band diagram between the region under the gate and the access region can lead to reflection of incident electrons.

**6 Conclusion** In conclusion, theoretical calculations for the mobility of electrons confined to a triangular well by an arbitrary electric field were done, and applied to an N-Polar HEMT. The drift mobility was measured with gated TLMs as a function of gate bias and found to match the experimental data well. It was shown through theory and measurements that increasing the electric field in the channel of a 2DEG has a detrimental effect on the mobility because the wave function is pushed closer to the barrier alloy. Furthermore, we observed an increase in the access resistance when the gate is reverse biased. This theoretical formalism can be applied to any other material system and

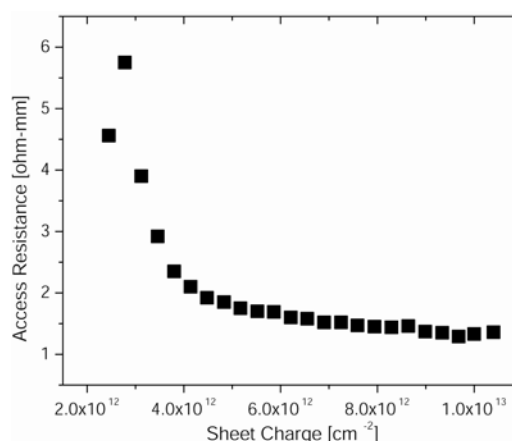


**Figure 4** Access resistance plotted vs. channel sheet charge as the device is reverse biased.

device structure in which a 2DEG is confined to a triangular well by a strong electric field.

**Acknowledgements** The authors gratefully acknowledge the support of Dr. Kitt Reinhardt and the AFOSR and the ONR-MINE program supervised by Dr. Paul Maki.

## References

- [1] F. Bernardini, V. Fiorentini, and D. Vanderbilt, *Phys. Rev. B* **56**, R10024 (1997).
- [2] R. Dimitrov, M. Murphy, J. Smart, W. Schaff, J. R. Shealy, L. F. Eastman, O. Ambacher, and M. Stutzmann, *J. Appl. Phys.* **87**, 3375 (2000).
- [3] S. Rajan, A. Chini, M. H. Wong, J. S. Speck, and U. K. Mishra, *J. Appl. Phys.* **102**, 044501 (2007).
- [4] S. Keller, C. S. Suh, Z. Chen, R. Chu, S. Rajan, N. A. Fichtenbaum, M. Furukawa, S. P. DenBaars, J. S. Speck, and U. K. Mishra *J. Appl. Phys.* **103**, 033708 (2008).
- [5] D. F. Brown, S. Rajan, S. Keller, Y. Hsieh, S. P. DenBaars, and U. K. Mishra, *Appl. Phys. Lett.* **93**, 042104 (2008).
- [6] B. Podor, CAS 1995 Proceedings, Sinaia, Romania, Oct. 11-14 1995.
- [7] Nidhi, S. Rajan, S. Keller, F. Wu, S. P. DenBaars, J. S. Speck and U. K. Mishra, *J. Appl. Phys.* **103**, 124508 (2008).
- [8] B. L. Gelmont, M. Shur, and M. Strosio, *J. Appl. Phys.* **77**, 657 (1994).
- [9] G. D. Bastard, *Wave-Mechanics applied to Semiconductor Heterostructures* 1st ed. (Les Editions de Physique, Les Ulis Cedex, France, 1991).
- [10] D. Jena, S. Heikman, J. S. Speck, A. Gossard, U. K. Mishra, A. Link, and O. Ambacher, *Phys. Rev. B* **67**, 153306 (2003).
- [11] M. Sumiya, K. Yoshimura, K. Ohtsuka, and S. Fuke, *Appl. Phys. Lett.* **76**, 2098 (2000).
- [12] J. H. Davies, *The Physics of Low-Dimensional Semiconductors*, 1st. ed. (Cambridge University Press, Cambridge, United Kingdom, 1998).